의학박사 학위 논문

다중형광염색 및 RNA 분석을 이용한 위장관 기질 종양의 포괄적 면역 프로파일링 분석: 티로신키나아제 치료의 종양 면역 미세 환경의 영향

Quantitative Multiplexed Immune Profiling of Advanced Gastrointestinal Stromal Tumors (GISTs): Impact of Tyrosine Kinase Inhibitors on the Tumor Immune Microenvironment

울 산 대 학 교 대 학 원

의 학 과

유 창 훈

다중형광염색 및 RNA 분석을 이용한 위장관 기질 종양의 포괄적 면역 프로파일링 분석: 티로신키나아제 치료의 종양 면역 미세 환경의 영향

지도교수: 강윤구

이 논문으로 의학 박사 학위 논문으로 제출함

2018년 12월

울산대학교 대학원

의학과

유창훈

유창훈의 의학박사학위 논문을 인준함

심사위원 김 병 식 (인)
심사위원 강 윤 구 (인)
심사위원 류 민 희 (인)
심사위원 김 경 미 (인)
심사위원 김 지 훈 (인)

울 산 대 학 교 대 학 원

2018년 12월

Table of Contents

Lists of Tables and Figures

영문요약

Background: The immune microenvironment of Gastrointestinal Stromal Tumors (GISTs) is largely unknown and there is no approved immunotherapeutic agent for the treatment of advanced GISTs. To investigate the potential application of novel immunotherapeutic strategies, we analyzed the immune microenvironment in tumors from patients with GISTs.

Methods: A total of 80 surgical specimens of advanced GISTs were acquired from 67 patients. The specimens were grouped according to the treatment setting: tyrosine kinase inhibitor (TKI)-naïve group (n=20); imatinib-progressed and no exposure to sunitinib or regorafenib (IM-PD group, n=30); and imatinib-progressed, sunitinib and/or regorafenib-treated group (IM-PD/SU-treated group, n=30). Seven-color multiplex immunofluorescence staining was performed on all 80 specimens. RNA sequencing and gene expression analysis for immune-related gene expression were performed on the specimens of 29 patients (TKI-naïve [n=10], IM-PD [n=14], and IM-PD/SU-treated group [n=5]).

Results: In TKI-naïve GISTs, the median number (interquartile range [IQR]) of immune cells per mm^2 was: CD3+, 79.2 (22.4-434.5); CD3+/CD8+, 6.7 (1.5-75.6); CD3+/FoxP3+, 4.4 (0.3-28.3); CD68+/CD204+, 2.3 (1.1-41.1); CD68+/CD204-, 8.7 (2.0-20.1); CD3+/PD1+, 0.6 (0-2.0); and CD3+/TIM3+, 0.2 (0-2.5). In IM-PD/SU-treated GISTs, the median number (IQR) of immune cells per mm^2 was: CD3+, 302.9 (63.4-502.9); CD3+/CD8+, 38.6 (8.9-105.4); CD3+/FoxP3+, 34.0 (6.6-59.7); CD68+/CD204+, 25.2 (6.4-54.2); CD68+/CD204-, 9.6 (4.0-28.9); CD3+/PD-1+, 2.3 (1.0-3.7); and CD3+/TIM3+, 1.8 (0-12.7). The regulatory T cells (CD3+/FoxP3+), M2 polarized macrophages (CD68+/CD204+), PD-1+ T cells (CD3+/PD-1+), and TIM3+ T cells (CD3+/TIM3+) were increased in the IM-PD/SU-treated group (P=0.047, P=0.023, P=0.016, and P=0.002, respectively).

IM-PD/SU-treated GISTs had increased ratios of infiltrative T cells to tumor cells (CD3+ cells per DOG-1+ cells, *P*=0.03); PD-1+ T-cells to pan-T cells (CD3+/PD-1+ per CD3+, *P*=0.002); PD-1+ cytotoxic T cells to pan-T cells (CD8+/PD-1+ per CD3+, *P*=0.007); PD-L1+ T-cell to pan-T cells (CD3+/PD-L1+ per CD3+, *P*=0.005); regulatory T cells to pan-T cells (CD3+/FoxP3+ per CD3+, *P*=0.006); and PD-1+ tumor cells to total tumor cells (DOG-1+/PD-1+ per DOG-1+, *P*=0.01). Compared to IM-PD GISTs, IM-PD/SU-treated GISTs had increased ratios of cytotoxic T cells to pan-T cells (CD3+/CD8+ per CD3+; *P*=0.07) and TIM3+ T cells to pan-T cells (CD3+/TIM3+ per CD3+; *P*=0.03). IM-PD/SU-treated GISTs had increased M2 polarized macrophages compared to TKI-naive GISTs (*P*=0.049) and marginally increased M2 polarized macrophages compared to IM-PD GISTs (*P*=0.10).

In the RNA sequencing (RNAseq) analysis, *FoxP3* expression was marginally increased in IM-PD/SU treated GISTs compared to TKI-naive GISTs (*P*=0.11). IM-PD/SU-treated GISTs had marginally increased *TIM3* expression compared to IM-PD GISTs (*P*=0.06). *TIGIT* expression was significantly increased in IM-PD/SU-treated GISTs compared to IM-PD GISTs (*P*=0.01).

Conclusion: Immune cell infiltrates were increased and immunosuppressive phenotypes were predominant in the tumors treated with anti-angiogenic agents compared to those that were TKI-naive or treated with imatinib. These findings suggest that this patient population may be appropriate candidates for future immunotherapy clinical trials targeting T cells or macrophages. Further investigation is needed to define optimal immunotherapy strategies in specific subpopulations of patients with GIST.

Introduction

Gastrointestinal stromal tumors (GISTs) are the most common mesenchymal tumors of the digestive tract, commonly occurring in the stomach and small intestine [1]. The molecular characteristics of GISTs include *KIT* or platelet-derived growth factor receptor alpha (*PDGFRA*) driver mutations, which are detectable in >90% of cases [1]. Although localized resectable disease is potentially curable with surgical resection only, the prognosis of patients with unresectable and/or metastatic GISTs was extremely poor before the emergence of imatinib (IM).

IM is an oral tyrosine kinase inhibitor (TKI) with activity against *KIT*, *PDGFRA*, *ABL*, and *DDR*. The efficacy of IM was first demonstrated in the pivotal B2222 trial [2], which showed in the extended follow-up report that the median time-to-progression (TTP) with IM was 2 years [3]. For patients with disease progression or intolerance of IM, sunitinib (SU) is the approved second-line therapy, with a median TTP of approximately 7 months as determined in the phase III trial [4]. Although many novel agents have been tested in the setting of failure of both IM and SU [5-7], regorafenib (REG) is the only drug approved as standard third-line therapy based on the success of a randomized phase III trial (GRID) that showed a median progression-free survival (PFS) of approximately 5 months in the REG arm [8]. For patients with refractory disease after failure of IM and SU, rechallenge of IM resulted in the significant delay of tumor progression compared to placebo in the RIGHT trial [9]. Despite progress in the management of advanced GISTs, current therapeutic strategies are mainly based on KIT inhibition. Major mechanism of acquired resistances on the approved TKIs is the development of secondary mutations in *KIT* or *PDGFRA*[10]. Although clinical trials of new TKIs targeting specific secondary resistance mutations are ongoing, these agents might be limited to improve the survival of overall patient population, considering the tumor heterogeneity of resistant

GISTs as multiple acquired secondary mutations are found in a single patient. Therefore, there are unmet medical needs for novel therapeutic approaches to improve the outcomes of patients with advanced GISTs.

Since ipilimumab, a CTLA-4 inhibitor, was approved for the management of advanced melanoma [11], immune checkpoint inhibitors such as anti-CTLA-4 and anti-PD-1/PD-L1 antibodies have led a paradigm shift in the management of advanced cancers; they have remarkably improved survival outcomes, particularly long-term survival [12, 13]. The United States (US) Food and Drug Administration (FDA) has approved immune checkpoint inhibitors for the management of various cancer types including melanoma, lung cancer, and hepatocellular carcinoma

However, there are few well-designed immunotherapy clinical trials for advanced GISTs and no immunotherapeutic agent has been approved for the management of GISTs. Considering that many immunotherapeutic strategies are now under development, evaluation of the immune microenvironment of advanced GISTs is essential for the successful incorporation of immunotherapy in the management of GISTs.

Materials and Methods

Patients

A total of 80 surgical specimens acquired from 67 patients with advanced GISTs were grouped according to three different treatment settings: TKI-naïve group (n=20); IM-progressed and no exposure to SU or REG (IM-PD group, n=30); and IM-progressed, SU and/or REG-treated group (IM-PD/SU-treated group, n=30). Multiplex immunofluorescence staining was performed on all 80 specimens and RNA sequencing (RNAseq) was performed on 29 specimens from patients in all treatment groups (TKI-naïve [n=10], IM-PD [n=14], and IM-PD/SU-treated [n=5]).

The study was approved by the Institutional Review Board of Asan Medical Center, Seoul, Korea, and conducted in accordance with the Declaration of Helsinki and Good Clinical Practice. Informed consent for immunohistochemistry analysis was obtained before enrollment in this study.

Multiplex immunofluorescence staining

Four-micrometer-thick whole-slide sections were obtained with a microtome and transferred onto positive charged slides, followed by multiplex immunofluorescence staining with a Leica Bond RxTM Automated Stainer (Leica Biosystems, Newcastle, UK). Briefly, the slides were baked for 30 min and dewaxed with Leica Bond Dewax solution (Cat #AR9222, Leica Biosystems, Milton Keynes, UK), followed by antigen retrieval with Bond Epitope Retrieval 2 (Cat #AR9640, Leica Biosystems, Milton Keynes, UK) in a pH 9.0 solution for 30 min.

Two panels were designed for multiplex immunofluorescence staining. Panel 1

contained DAPI (Opal™ 7-color Manual IHC Kit; Perkin Elmer, Waltham, MA, USA), DOG-1 (244R-15; Cell Marque, Austin, TX, USA), CD3 (790-4341; Ventana, Tucson, AZ, USA), CD8 (MCA1817; AbD Serotec, Oxford, UK), FOXP3 (ab20034; Abcam, Cambridge, MA, USA), PD-1 (ab137132; Abcam, Cambridge, MA, USA), and PD-L1 (13684; CST, Danvers, MA, USA). Panel 2 contained DAPI, DOG-1, CD3, TIM3 (45208S; CST, Danvers, MA, USA), CD68 (M0876; Dako, Carpinteria, CA, USA), and CD204 (KT022; TransGenic, Kumamoto, Japan) (Figure 1).

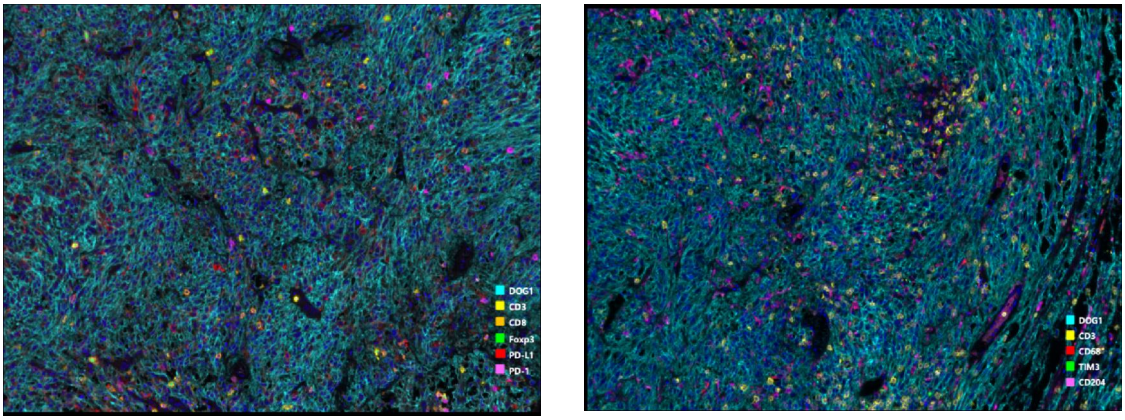

Panel 1 Panel 2

Figure 1. Representative images for panel 1 and panel 2

Each section was subjected to five sequential rounds of staining, each including a protein block with PKI blocking/antibody diluent, followed by incubation with primary antibody and a corresponding secondary horseradish peroxidase-conjugated polymer using the OpalTM Polymer HRP Ms+ Rb kit (Perkin Elmer, Waltham, MA, USA). Each horseradish peroxidase-conjugated polymer mediated the covalent binding of a different fluorophore using TSA. This covalent reaction was followed by additional antigen retrieval with Bond Epitope Retrieval 1 (Cat #AR9961; Leica Biosystems, Milton Keynes, UK) for 20 min to remove bound antibodies before the next step in the sequence. After five sequential reactions, sections were

counterstained with DAPI and coverslips were applied using HIGHDEF® IHC Fluoromount (Enzo Life Sciences, Farmingdale, NY, USA).

Multispectral imaging

Multiplex stained slides were scanned using the Vectra® Multispectral Imaging System version 3 (Perkin Elmer, Boston, MA, USA). Each 200 X multispectral image cube was created by combining images obtained at 10 nm intervals of the emission light spectrum across the range of each emission filter cube. The filter cubes used for multispectral imaging were DAPI (440–680 nm), FITC (520–680 nm), Cy3 (570–690 nm), Texas Red (580–700 nm), and Cy5 (670–720 nm). In each slide, 8 to 11 regions of interest (ROIs) were selected and analyzed. The average values of the analyzed ROIs were used for the analysis.

RNAseq and gene set enrichment analysis (GSEA)

Total RNA was extracted using RNeasy with QIAshredders (Qiagen). RNA quality was assessed by analysis of rRNA band integrity on an Agilent RNA 6000 Nano kit (Agilent Technologies, CA). Before cDNA library construction, 1 ug of total RNA and magnetic beads with Oligo (dT) were used to enrich for poly (A) mRNA. Then, the purified mRNA was disrupted into short fragments, and double-stranded cDNA was immediately synthesized. The cDNA was subjected to end-repair and poly (A) addition and connected with sequencing adapters using the TruSeq RNA sample prep Kit (Illumina, CA). The suitable fragments automatically purified by BluePippin 2% agarose gel cassette (Sage Science, MA) were selected as templates for PCR amplification. The final library sizes and qualities were evaluated electrophoretically with an Agilent High Sensitivity DNA kit (Agilent Technologies, CA); the fragment was found to be between 350–450 bp. Subsequently, the library was sequenced using an Illumina HiSeq2500 sequencer (Illumina, CA).

Gene expression level was measured with Cufflinks v2.1.1 using the gene annotation database of Ensembl release 77. The noncoding gene region was removed using the –mask option. To improve the measurement accuracy, multi-read-correction and fragbias-correct options were applied. The '-max-bundle-frags' option was set to 10,000,000 to estimate the highly expressed genes. All other options were set to default values. Differentially expressed genes were identified using the Cuffdiff tool with the default parameter setting at a significance level of $P < 0.05$.

GSEA is a computational methodology to identify classes of genes that are overexpressed in a large set of genes between PD-L1 low and PD-L1 high cell lines (A549 with PD-L1 overexpression versus control; H522 with PD-L1 knockdown versus control). This analysis was done using GenePattern (https:// genepattern.broadinstitute.org/). The Molecular Signatures Database (MSigDB) C2 collection, consisting of canonical pathways and experimental signatures curated from publications, was used for the analysis.

Statistical analysis

Continuous variables and proportions were compared using the independent T, Mann–Whitney U, Chi-square, or Fisher's exact test, as appropriate. To assess the associations among the data, Pearson's correlation coefficient was used. The mean levels of ther markers among three patient groups were compared using analysis of variance (ANOVA). Two-tailed *P* values < 0.05 were considered statistically significant. All statistical analyses were performed using SPSS 22.0 software (SPSS Inc., Chicago, IL, USA).

Results

Patients

The patients' baseline characteristics are summarized in Table 1. The median age of the patients included in this analysis was 55 years (range, 31-76 years) and 61% were male. Small bowel was the most common primary site (n=42, 63%), followed by stomach (n=24, 36%). In 63 patients whose primary genotype was evaluated, *KIT* exon 11 deletion was most common (n=35, 56%), followed by *KIT* exon 9 mutation (n=11, 18%), *KIT* exon 11 mutation except deletion (n=10, 16%), and *PDGFRA* exon 18 mutation (n=2, 3%). There were no significant differences among the groups with regard to sex (*P*=0.49), age (*P*=0.29), or primary genotype (*P*=0.08); the only difference was the primary tumor site (*P*=0.047).

Table 1. Patients' baseline characteristics

Variables	TKI-naïve group (n=20)	IM-PD group (n=30)	IM-PD/SU-treated group (n=30)
Age, years (range)	54 (32-74)	60 (32-76)	50 (31-70)
Sex			
Male	15 (75%)	18 (60%)	18 (60%)
Female	5 (25%)	12 (40%)	12 (40%)
Primary tumor site			
Stomach	9 (45%)	14 (47%)	5 (17%)
Small bowel	11 (55%)	16 (53%)	24 (80%)
Others	0	0	1 (3%)
Genotype			
KIT exon 11 deletion	7 (35%)	20 (67%)	13 (43%)
KIT exon 11 no deletion	3 (15%)	4 (13%)	5 (17%)
KIT exon 9 mutation	3 (15%)	4 (13%)	6 (20%)
PDGFRA exon 18 mutation	1 (5%)	0	1 (3%)
Wild type KIT/PDGFRA	4 (20%)	1 (3%)	2 (7%)

Not available	2 (10%)	1 (3%)	3 (10%)

TKI=tyrosine kinase inhibitor, IM-PD group= imatinib-progressed and no exposure to sunitinib/or regorafenib, IM-PD/SU-treated group=imatinib-progressed and received sunitinib and/or regorafenib

Correlation between the indicators for tumor immune microenvironment

We performed correlative analysis between the markers for tumor immune microenvironment for all 80 specimens (Figure 2-3). The number of cytotoxic T cells (CD3+/CD8+) was positively correlated with the number of regulatory T cells (CD3+/FoxP3+; Figure 2A; R^2=0.63, *P*<0.001), PD-1+ T-cells (CD3+/PD-1+; Figure 2B; R^2=0.66, *P*<0.001), PD-1+ tumor cells (DOG-1+/PD-1+: Figure 2C: R^2=0.57, *P*<0.001), and TIM3+ T cells (CD3+/TIM3+: Figure 2D: R^2=0.43, *P*<0.001). The number of regulatory T cells was positively correlated with the number of PD-1+ T cells (Figure 2E: R^2=0.56, *P*<0.001), PD-1+ tumor cells (Figure 2F: R^2=0.51, *P*<0.001), and TIM3+ T cells (Figure 2G: R^2=0.37, *P*<0.001). The number of TIM3+ T cells also positively correlated with the number of PD-1+ and PD-L1+ tumor cells (R^2=0.35, *P*<0.001 and R^2=0.21, *P*=0.02, respectively).

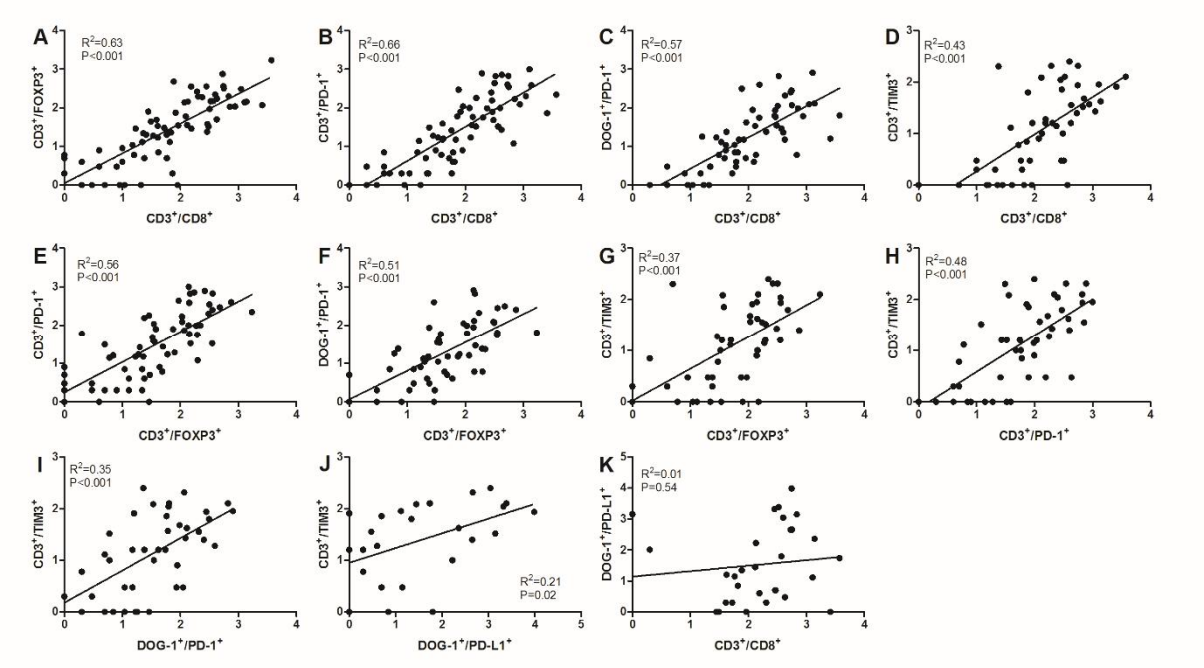

Figure 2. Correlative analysis between the markers for tumor immune microenvironment

In the analyses of the relationship between macrophage and other tumor immune microenvironment markers (Figure 3), the number of CD68+ (pan-macrophage) and CD204 (M2-polarized) cells positively correlated with the number of pan-T cells (CD3+: R^2=0.18, *P*<0.001; Figure 3A and R^2=0.11, *P*=0.003; Figure 3B, respectively) and cytotoxic T cells (CD3+/CD8+: R^2=0.30, *P*<0.001; Figure 3C and R^2=0.27, *P*<0.001; Figure 3D, respectively). M2 polarized macrophages (CD68+/CD204+) positively correlated with cytotoxic T cells (CD3+/CD8+: R^2=0.14, *P*=0.001; Figure 3E), PD-1+ T cells (CD3+/PD-1+: R^2=0.22, *P*<0.001; Figure 3G), and PD-1+ tumor cells (DOG-1+/PD-1+: R^2=0.10, *P*=0.02; Figure 3I). M1 polarized macrophages (CD68+/CD204-) significantly correlated with cytotoxic T cells (R^2=0.31, *P*<0.001; Figure 3F) and PD-1+ T cells (R^2=0.39, *P*<0.001; Figure 3H). There was also a positive relationship between M2 and M1 polarized macrophages (R^2=0.39, *P*<0.001; Figure 3K).

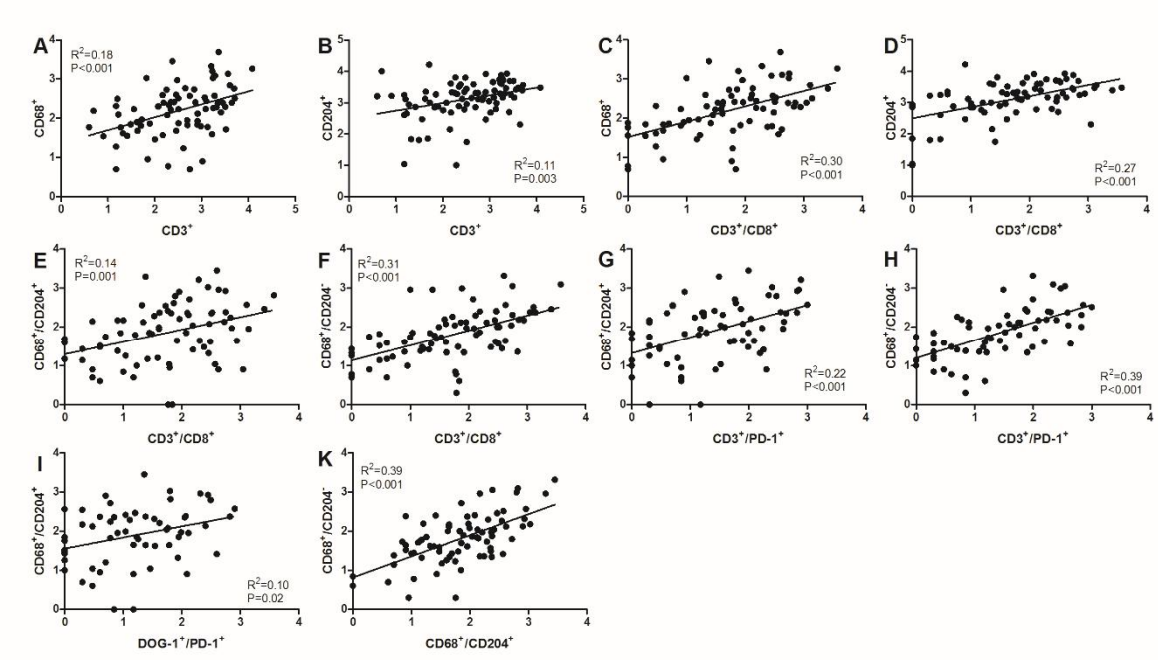

Figure 3. Correlative analysis between macrophage and other tumor immune microenvironment markers

Immune microenvironment of TKI-naive GIST using multiplex immunofluorescence staining

We analyzed the immune microenvironment of the 20 surgical specimens from the patients with TKI-naive GIST (see the summary in Tables 2 and 3). The median number (interquartile range [IQR]) of immune cells per mm^2 was: CD3+, 79.2 (22.4-434.5); CD3+/CD8+, 6.7 (1.5-75.6); CD3+/FoxP3+, 4.4 (0.3-28.3); CD68+/CD204+, 2.3 (1.1-41.1); CD68+/CD204-, 8.7 (2.0-20.1); CD3+/PD1+, 0.6 (0-2.0); and CD3+/TIM3+, 0.2 (0-2.5).

The median cytotoxic T cell ratio (CD3+/CD8+ cells per CD3+ cells) was 13.2% (range, 0%-52.1%), and the median regulatory T cell ratio (CD3+/FoxP3+ cells per CD3+ cells) was 3.0% (range, 0%-34.0%). The median ratios of infiltrative T cells to tumor cells (CD3+ cells per DOG-1+ cells), PD-1+ T cells to pan-T cells (CD3+/PD-1+ cells per CD3+ cells), and TIM3+ T cells to pan T-cells (CD3+/TIM3+ cells per CD3+ cells) were 1.8% (range, 0.2%-100%), 2.1% (range, 0%-38.1%) and 16.0% (range, 0%-250.0%), respectively. The median tumor PD-L1+ (DOG-1+/PD-L1+ cells per DOG-1+ cells) and PD-1+ (DOG-1+/PD-1+ per DOG-1+) rates were 0% (range, 0%-0.8%) and 0% (range, 0%-0.7%), respectively. The median M1 and M2 polarized macrophage to tumor cells ratios (CD68+/CD204- cells per DOG-1+ cells and CD68+/CD204+ cells per DOG-1+ cells, respectively) were 52.5% (range, 2.0%-1242.0%) and 15.5% (range, 0%-907.0%), respectively.

Table 2. Immune cell subpopulation according to the clinical setting

Clinical setting	All (n=80), median (IQR 25%-75%)	TKI-naïve group (n=20), median (IQR 25%-75%)	IM-PD group (n=30), median (IQR 25%-75%)	IM-PD/SU-treated group (n=30), median (IQR 25%-75%)	*P* value
CD3+ cells	92.6 (22.6-449.3)	79.2 (22.4-434.5)	43.5 (11.3-239.9)	302.9 (63.4-502.9)	0.18
CD3+/CD8+ cells	14.0 (2.6-73.2)	6.7 (1.5-75.6)	6.4 (0.8-25.9)	38.6 (8.9-105.4)	0.13
CD3+/FoxP3+ cells	6.6 (1.0-34.0)	4.4 (0.3-28.3)	2.4 (0.3-8.1)	34.0 (6.6-59.7)	0.047
CD68+/CD204+ cells	9.7 (2.5-31.4)	2.3 (1.1-41.1)	8.5 (2.9-19.2)	25.2 (6.4-54.2)	0.023
CD68/CD204- cells	8.7 (3.7-19.3)	8.7 (2.0-20.1)	7.5 (3.6-15.2)	9.6 (4.0-28.9)	0.18
CD3+/PD-1+ cells	1.0 (0.3-2.8)	0.6 (0-2.0)	0.6 (0-1.5)	2.3 (1.0-3.7)	0.016
CD3+/TIM3+ cells	0.2 (0-2.3)	0.2 (0-2.5)	0.1 (0-0.5)	1.8 (0-12.7)	0.002

*Values are expressed as number of cells per mm^2

TKI=tyrosine kinase inhibitor, IM-PD group= imatinib-progressed and no exposure to sunitinib/or regorafenib, IM-PD/SU-treated group=imatinib-progressed and received sunitinib and/or regorafenib

Table 3. Immune microenvironment according to the clinical setting

Clinical setting	TKI-naïve group, median (range)	IM-PD group, median (range)	IM-PD/SU-treated group, median (range)	*P* value
CD3+/CD8+ cells/CD3+ cells	13.2% (0-52.1%)	13.9% (0-30.0%)	17.3% (4.5-45.6%)	0.14
CD3+/FoxP3+ cells/CD3+ cells	3.0% (0-34.0%)	4.9% (0-23.1%)	12.7% (2.1-42.8%)	0.006
CD3+ cells/DOG-1+ cells	1.8% (0.2-100%)	1.0% (0-12.5%)	3.5% (0.1-32080.0%)	0.03
CD3+/PD-1+ cells/CD3+ cells	2.1% (0-38.1%)	2.0% (0-37.5%)	9.6% (0-56.7%)	0.002
DOG-1+/PD-L1+ cells/DOG-1+ cells	0% (0-0.8%)	0% (0-4.5%)	0% (0-39.6%)	0.05
DOG-1+/PD-1+ cells/DOG-1+ cells	0% (0-0.7%)	0% (0-9.1%)	0.1% (0-1.8%)	0.01
CD3+/TIM3+ cells/CD3+ cells	1.5% (0-127.0%)	1.0% (0-72.0%)	16.0% (0-250.0%)	0.07
CD68+/CD204+ cells/DOG-1+ cells	15.5% (0-907.0%)	52.5% (0-802.0%)	194.0% (1.0-2818.0%)	0.09
CD68+/CD204- cells/DOG-1+ cells	52.5% (2.0-1242.0%)	50.0% (0-914.0%)	92.0% (0-2071.0%)	0.88
PD-1+ tumor cell rate > 1%, n (%)	0 (0%)	1 (3.3%)	3 (10.0%)	0.32
PD-L1+ tumor cell rate > 1%, n	0 (0%)	1 (3.3%)	3 (10.0%)	0.32

(%)				
PD-1+ T-cell rate > 1%, n (%)	13 (65.0%)	20 (66.7%)	27 (90.0%)	0.06
PD-L1+ T-cell rate > 1%, n (%)	1 (5.0%)	0 (0%)	8 (26.7%)	0.003

TKI=tyrosine kinase inhibitor, IM-PD group= imatinib-progressed and no exposure to sunitinib/or regorafenib, IM-PD/SU-treated group=imatinib-progressed and received sunitinib and/or regorafenib

Immune microenvironment of GISTs in different clinical settings using multiplex immunofluorescence staining

The immune microenvironments of GISTs were compared according to the different clinical settings (TKI-naive vs IM-PD vs IM-PD/SU-treated) (Figure 4-5 and Table 2-3). There were no significant differences between the immune cell subpopulations of the TKI-naive and IM-PD groups.

The median number (IQR) of immune cells per mm^2 in the specimens from the IM-PD/SU-treated group was: CD3+, 302.9 (63.4-502.9); CD3+/CD8+, 38.6 (8.9-105.4); CD3+/FoxP3+, 34.0 (6.6-59.7); CD68+/CD204+, 25.2 (6.4-54.2); CD68+/CD204-, 9.6 (4.0-28.9); CD3+/PD-1+, 2.3 (1.0-3.7); and CD3+/TIM3+, 1.8 (0-12.7). The number of regulatory T cells (CD3+/FoxP3+), M2 polarized macrophages (CD68+/CD204+), PD-1+ T cells (CD3+/PD-1+), and TIM3+ T cells (CD3+/TIM3+) was increased in the IM-PD/SU-treated group (P=0.047, P=0.023, P=0.016, and P=0.002, respectively) among three groups.

IM-PD/SU-treated GISTs had increased ratios of infiltrative T cells to tumor cells (CD3+ cells per DOG-1+ cells; P=0.03; Figure 4A); PD-1+ T-cells to pan-T cells (CD3+/PD-1+ per CD3+; P=0.002; Figure 4C); PD-1+ cytotoxic T-cells to pan-T cells (CD8+/PD-1+ per CD3+; P=0.007; Figure 4D); PD-L1+ T-cells to pan-T cells (CD3+/PD-L1+ per CD3+; P=0.005; Figure E); regulatory T-cells to pan-T cells (CD3+/FoxP3+ per CD3+; P=0.006; Figure 4F), and PD-1+ tumor cells to total tumor cells (DOG-1+/PD-1+ per DOG-1+; P=0.01; Figure 4G) among three groups. Compared to IM-PD GISTs, IM-PD/SU-treated GISTs had an increased cytotoxic T cell to pan-T cell ratio (CD3+/CD8+ per CD3+; P=0.07) and TIM3+ T cell to pan T cell ratio (CD3+/TIM3+ per CD3+; P=0.03).

There was no difference in the pan-macrophage per tumor cell ratio (P=0.43, Figure 5A) and the M1 polarized macrophage per tumor cell ratio (P=0.68; Figure 5C). IM-PD/SU-treated GISTs had increased M2 polarized macrophages compared to TKI-naive GISTs (P=0.049, Figure 5B) and marginally increased M2 polarized macrophages compared to IM-PD GISTs (P=0.10).

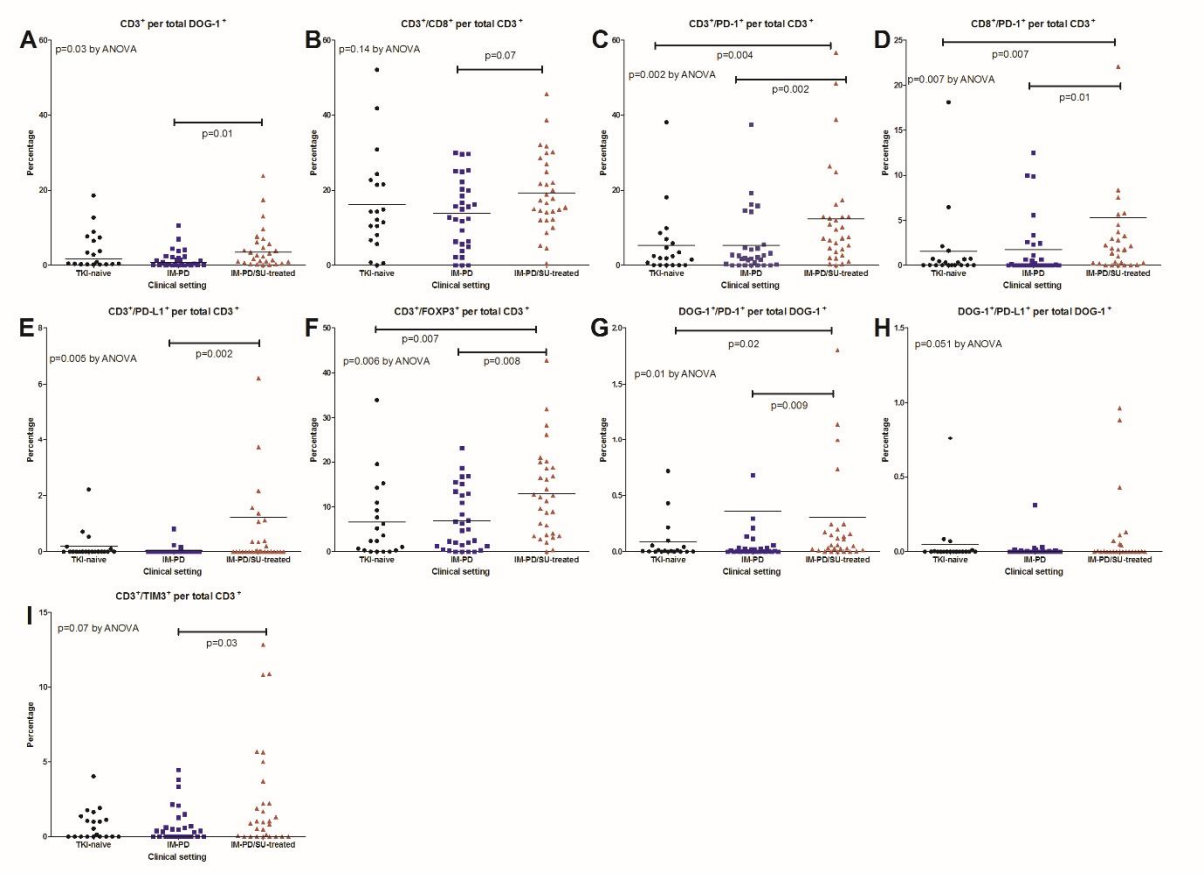

Figure 4. Tumor immune microenvironment according to the different clinical settings

TKI=tyrosine kinase inhibitor, IM-PD group= imatinib-progressed and no exposure to sunitinib/or regorafenib, IM-PD/SU-treated group=imatinib-progressed and received sunitinib and/or regorafenib

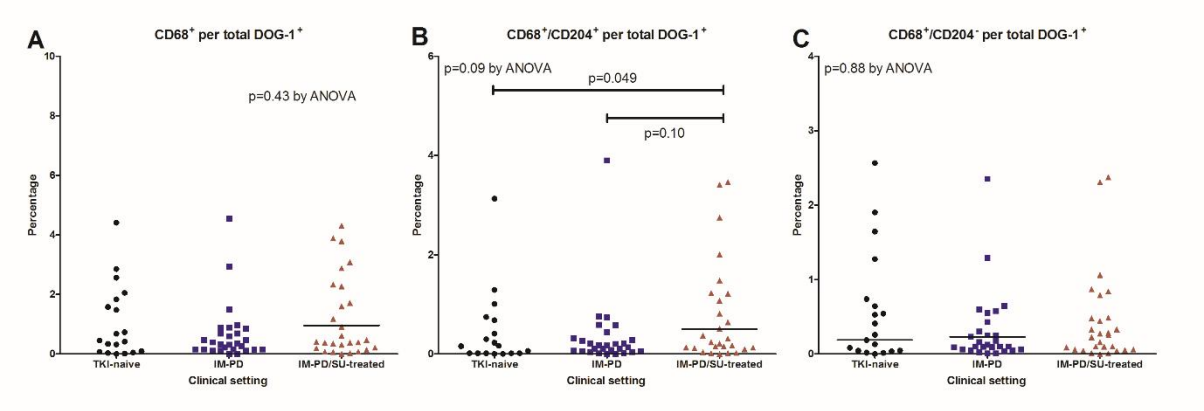

Figure 5. Tumor associated macrophage infiltration according to the different clinical settings

TKI=tyrosine kinase inhibitor, IM-PD group= imatinib-progressed and no exposure to sunitinib/or regorafenib, IM-PD/SU-treated group=imatinib-progressed and received sunitinib and/or regorafenib

Gene expression analysis using RNAseq in different clinical settings

RNAseq was performed for TKI-naive (n=10), IM-PD (n=14), and IN-PD/SU-treated GISTs (n=5). The results of gene expression analysis using RNAseq on specimens from patients in the different clinical settings are depicted in Figure 6. While *FoxP3* expression was marginally increased in IM-PD/SU-treated GISTs compared to TKI-naive GISTs (*P*=0.11; Figure 6C) and IM-PD/SU-treated GISTs had a marginal increase in *TIM3* expression compared to IM-PD GISTs (*P*=0.06; Figure 6E), *TIGIT* expression was significantly increased in IM-PD/SU-treated GISTs compared to IM-PD GISTs (*P*=0.01; Figure 6F). There was a trend towards decreased interferon gamma gene expression (*P*=0.07) in IM-PD/SU-treated GISTs compared to TKI-naive GISTs (Figure 7).

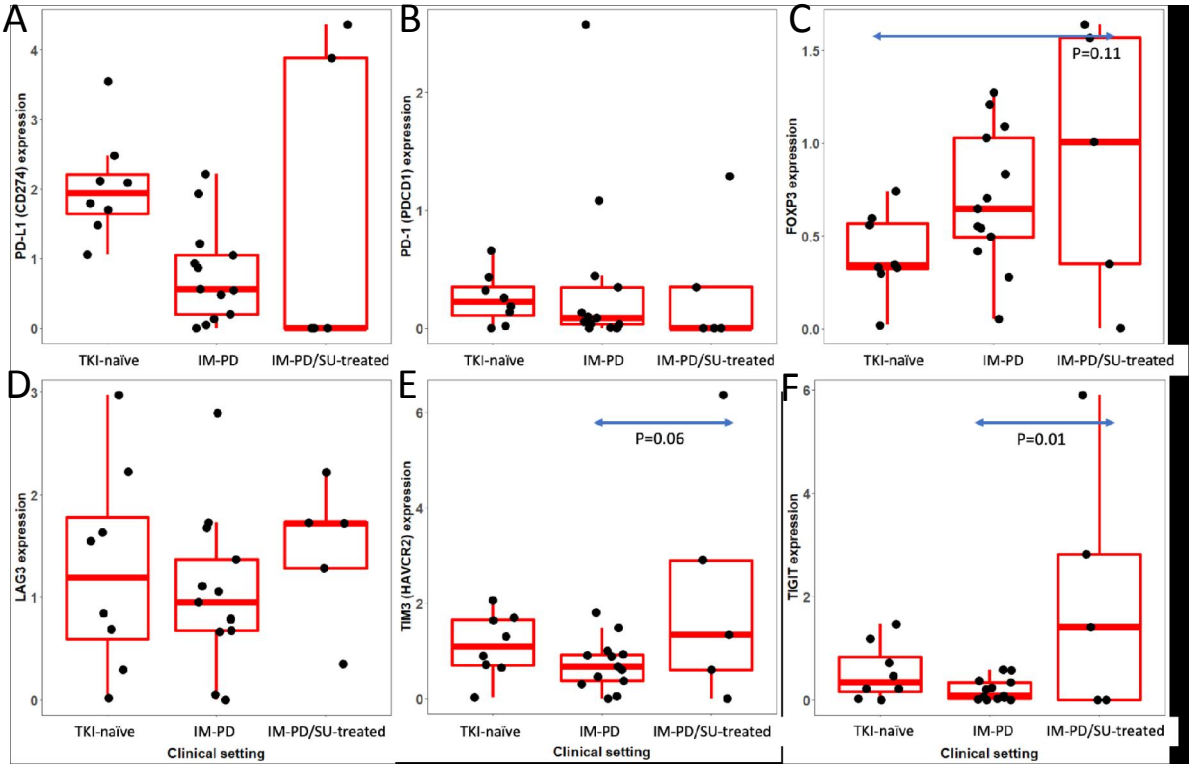

Figure 6. Gene expression analysis using RNAseq according to the different clinical settings

TKI=tyrosine kinase inhibitor, IM-PD group= imatinib-progressed and no exposure to sunitinib/or regorafenib, IM-PD/SU-treated group=imatinib-progressed and received sunitinib and/or regorafenib

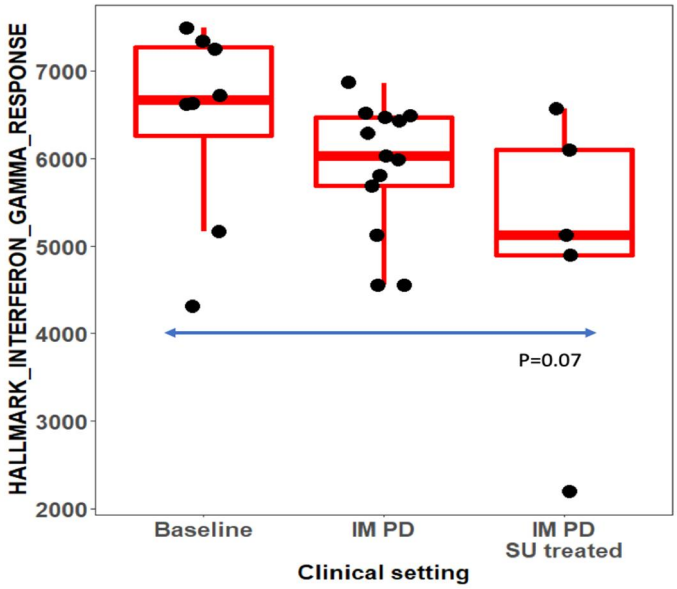

Figure 7. Interferon gamma gene signature analysis according to the different clinical settings

Baseline=tyrosine kinase inhibitor-naïve group, IM-PD group= imatinib-progressed and no exposure to sunitinib/or regorafenib, IM-PD/SU-treated group=imatinib-progressed and received sunitinib and/or regorafenib

Discussion

Our analysis showed that GISTs harbor T cell and macrophage infiltrates. The amount of T cell infiltration was significantly associated with an immunosuppressive phenotype including regulatory T cells, PD-1+ T cells, and TIM-3+ T cells. Tumor PD-1 expression also correlated with an immunosuppressive T cell phenotype including regulatory T cells and TIM3+ T cells.

The numbers of infiltrating pan-T cells (CD3+ cells) and macrophages (CD68+ cells) in TKI-naive GISTs were comparable to those reported previously [14]. However, cytotoxic T cells (CD3+/CD8+), T cells with exhausted phenotype (regulatory T cells [CD3+/FoxP3+], PD-1+ T cells, and TIM3+ T cells) were scarce in TKI-naive GISTs. This seems to conflict with the results of a previous study that showed that tumor PD-L1 expression (29%) and lymphocyte PD-L1 expression (50%) are relatively common in GISTs [15]. However, the discrepancies between the studies may due to variability in the PD-L1 assays and other assessment methodologies [15]. This also might reflect the differences among patient populations. All tumor specimens in our TKI-naive group were from the patients who later progressed, while a previous study suggests that immune cells are more highly infiltrated in localized tumors with good prognosis [16].

Consistent with the clinical setting, although there were no significant differences between the immune cell subpopulations of TKI-naive GISTs and IM-PD GISTs, the anti-angiogenic agent-treated group (i.e., the IM-PD/SU-treated group) showed a different profile of increased T-cell infiltration and exhausted T-cell phenotype compared to the TKI-naive and IM-PD groups. These findings indicate that patients with GISTs who progressed on IM and then, received SU, or REG may be potential candidates for future clinical trials of immune

checkpoint inhibitors against advanced GISTs.

It is not clear whether the differences in immune profiles that we observed were the result of the natural course of the disease. However, considering that there were no significant differences between the immune profiles of TKI-naive GISTs and IM-PD GISTs, the increased T cell infiltration in the tumors and exhausted T cell phenotype in the IM-PD/SU-treated group may have been induced by the treatment with anti-angiogenic agents, including SU or REG. Recent studies have shown that anti-angiogenic agents promote T-cell infiltration into tumors [17]. In addition, anti-angiogenic agents may have a role in enhancing the efficacy of immunotherapy via reversing the immunosuppressive tumor microenvironment [18-20].

Our analysis also showed increased M2 polarized macrophages in IM-PD/SU-treated GISTs compared to TKI-naive or IM-PD GISTs, while there were no differences in pan-macrophages and M1 polarized macrophages among the different clinical settings. These results are consistent with the results of previous studies showing that M2 polarized macrophages are more prominent in TKI-treated GISTs compared to TKI-naive GISTs [14]. Macrophages with an M2 phenotype are known to have anti-inflammatory effects and consist mostly of tumor-associated macrophages (TAM) [21]. M2 polarized macrophages also exhibit functions that may help tumor progression and have been negatively correlated with survival outcomes in patients with advanced solid tumors [22, 23]. As previous research showed that M2 polarized macrophages are more commonly found in metastatic GISTs compared to primary lesions, increased M2 polarized macrophages in IM-PD/SU-treated GISTs may be related to the tumor progression itself [14]. However, considering the interaction between macrophage polarization and angiogenesis, the potential impact of SU or REG on this phenomenon cannot be excluded [24].

Although immunotherapy, particularly immune checkpoint inhibitors including anti-PD-1/PD-L1 inhibitors or anti-CTLA-4 inhibitors, has changed the therapeutic landscape for multiple cancer types, the major therapeutic strategy against advanced GISTs remains to inhibit c-KIT via IM, SU, and REG. Although several small trials using immune checkpoint inhibitors such as nivolumab, nivolumab plus ipilimumab, and ipilimumab plus dasatinib have been conducted for patients with advanced GISTs, the outcomes of these trials were not successful [25]. On the basis of our current findings, immune checkpoint inhibitors or combination therapy with multiple immune checkpoint inhibitors for GIST patients previously treated with anti-angiogenic agents may be a valuable investigational strategy, as PD-1, TIM3, and TIGIT are overexpressed in this patient population. Considering the immune modulating effect of anti-angiogenic agents in GISTs demonstrated in our study, combination therapy with immune checkpoint inhibitors and anti-angiogenic agents may also be a potential approach to enhance the efficacy of immune checkpoint inhibitors in advanced GISTs, as this strategy has shown successful preliminary outcomes in advanced hepatocellular carcinoma. The interferon gamma gene signature, a potential predictor for the efficacy of anti-PD-1/PD-L1 inhibitors [26], was decreased in the IM-PD/SU-treated GISTs compared to other groups. Although only 5 patients treated with anti-angiogenic agents were included in the RNAseq analysis, this finding suggests that combination therapy may be favored over anti-PD-1/PD-L1 inhibitor monotherapy for future clinical trials. In addition to T cell targeted immunotherapy, targeting tumor-associated macrophages via CCR2, CSF1R, or CD40 also might be effective in GIST patients previously treated with anti-angiogenic agents, as these agents have shown promising preliminary outcomes in other cancer types [27-29].

In conclusion, immune cell infiltrates were increased and immunosuppressive

phenotypes were predominant in the tumors from patients treated with anti-angiogenic agents compared to those from patients that were TKI-naive or treated with IM only. These findings suggest that this patient population may be appropriate candidates for future immunotherapy clinical trials targeting T cells or macrophages. Further investigation is needed to define optimal immunotherapy strategies in specific subpopulations of patients with GIST.

References

1. Joensuu H, Hohenberger P, Corless CL. Gastrointestinal stromal tumour. The Lancet 2013:1–11.

2. Demetri GD, Mehren von M, Blanke CD et al. Efficacy and safety of imatinib mesylate in advanced gastrointestinal stromal tumors. N Engl J Med 2002; 347(7):472–480.

3. Blanke CD, Demetri GD, Mehren von M et al. Long-Term Results From a Randomized Phase II Trial of Standard- Versus Higher-Dose Imatinib Mesylate for Patients With Unresectable or Metastatic Gastrointestinal Stromal Tumors Expressing KIT. J. Clin. Oncol. 2008; 26(4):620–625.

4. Demetri GD, van Oosterom AT, Garrett CR et al. Efficacy and safety of sunitinib in patients with advanced gastrointestinal stromal tumour after failure of imatinib: a randomised controlled trial. Lancet 2006; 368(9544):1329–1338.

5. Kang YK, Yoo C, Ryoo BY et al. Phase II study of dovitinib in patients with metastatic and/or unresectable gastrointestinal stromal tumours after failure of imatinib and sunitinib. Br. J. Cancer 2013; 109(9):2309–2315.

6. Judson I, Scurr M, Gardner K et al. Phase II Study of Cediranib in Patients with Advanced Gastrointestinal Stromal Tumors or Soft-Tissue Sarcoma. Clinical Cancer Research 2014; 20(13):3603–3612.

7. Dickson MA, Okuno SH, Keohan ML et al. Phase II study of the HSP90-inhibitor BIIB021 in gastrointestinal stromal tumors. Annals of Oncology 2012; 24(1):252–257.

8. Demetri GD, Reichardt P, Kang Y-K et al. Efficacy and safety of regorafenib for advanced gastrointestinal stromal tumours after failure of imatinib and sunitinib (GRID): an international, multicentre, randomised, placebo-controlled, phase 3 trial. Lancet 2013; 381(9863):295–302.

9. Kang Y-K, Ryu M-H, Yoo C et al. Resumption of imatinib to control metastatic or unresectable gastrointestinal stromal tumours after failure of imatinib and sunitinib (RIGHT): a randomised,placebo-controlled, phase 3 trial. Lancet Oncology 2013; 14(12):1175–1182.

10. Antonescu CR, Besmer P, Guo T et al. Acquired resistance to imatinib in gastrointestinal stromal tumor occurs through secondary gene mutation. Clin. Cancer Res. 2005; 11(11):4182–4190.

11. Robert C, Thomas L, Bondarenko I et al. Ipilimumab plus dacarbazine for previously untreated metastatic melanoma. N Engl J Med 2011; 364(26):2517–2526.

12. Wolchok JD, Kluger H, Callahan MK et al. Nivolumab plus Ipilimumab in Advanced Melanoma. N Engl J Med 2013; 369(2):122–133.

13. Robert C, Schachter J, Long GV et al. Pembrolizumab versus Ipilimumab in Advanced Melanoma. N Engl J Med 2015; 372(26):2521–2532.

14. van Dongen M, Savage NDL, Jordanova ES et al. Anti-inflammatory M2 type macrophages characterize metastasized and tyrosine kinase inhibitor-treated gastrointestinal stromal tumors. Int. J. Cancer 2010; 122:NA–NA.

15. D'Angelo SP, Shoushtari AN, Agaram NP et al. Prevalence of tumor-infiltrating lymphocytes and PD-L1 expression in the soft tissue sarcoma microenvironment. Human Pathology 2015; 46(3):357–365.

16. Rusakiewicz S, Semeraro M, Sarabi M et al. Immune Infiltrates Are Prognostic Factors in Localized Gastrointestinal Stromal Tumors. Cancer Res. 2013; 73(12):3499–3510.

17. Bendell JC, Funke R, Sznol M et al. Atezolizumab in combination with bevacizumab enhances antigen-specific T-cell migration in metastatic renal cell carcinoma. Nat Comms 2016; 7(1):1–8.

18. Motz GT, Santoro SP, Wang L-P et al. Tumor endothelium FasL establishes a selective immune barrier promoting tolerance in tumors. Nat Med 2014; 20(6):607–615.

19. Hegde PS, Wallin JJ, Mancao C. Predictive markers of anti-VEGF and emerging role of angiogenesis inhibitors as immunotherapeutics. Seminars in Cancer Biology 2018; 52(Part 2):117–124.

20. Goel S, Duda DG, Xu L et al. Normalization of the Vasculature for Treatment of Cancer and Other Diseases. Physiological Reviews 2011; 91(3):1071–1121.

21. Brown JM, Recht L, Strober S. The Promise of Targeting Macrophages in Cancer Therapy. Clin. Cancer Res. 2017; 23(13):3241–3250.

22. Steidl C, Lee T, Shah SP et al. Tumor-associated macrophages and survival in classic Hodgkin's lymphoma. N Engl J Med 2010; 362(10):875–885.

23. Ostuni R, Kratochvill F, Murray PJ, Natoli G. Macrophages and cancer: from mechanisms to therapeutic implications. Trends in Immunology 2015; 36(4):229–239.

24. De Palma M, Biziato D, Petrova TV. Microenvironmental regulation of tumour angiogenesis. Nat Rev Cancer 2017; 17(8):457–474.

25. D'Angelo SP, Shoushtari AN, Keohan ML et al. Combined KIT and CTLA-4 Blockade in Patients with Refractory GIST and Other Advanced Sarcomas: A Phase Ib Study of Dasatinib Plus Ipilimumab. Clin. Cancer Res. 2016. doi:10.1158/1078-0432.CCR-16-2349.

26. Cogdill AP, Andrews MC, Wargo JA. Hallmarks of response to immune checkpoint blockade. Br. J. Cancer 2017; 117(1):1–7.

27. Beatty GL, Chiorean EG, Fishman MP et al. CD40 Agonists Alter Tumor Stroma and Show Efficacy Against Pancreatic Carcinoma in Mice and Humans. Science 2011; 331(6024):1612–1616.

28. Zhu Y, Knolhoff BL, Meyer MA et al. CSF1/CSF1R Blockade Reprograms Tumor-Infiltrating Macrophages and Improves Response to T-cell Checkpoint Immunotherapy in Pancreatic Cancer Models. Cancer Res. 2014; 74(18):5057–5069.

29. Nywening TMN, Wang-Gillam AW-G, Sanford DES et al. Targeting tumour-associated macrophages with CCR2 inhibition in combination with FOLFIRINOX in patients with borderline resectable and locally advanced pancreatic cancer: a single-centre, open-label, dose-finding, non-randomised, phase 1b trial. Lancet Oncology 2016; 17(5):651–662.

국문요약

배경: 위장관 기질종양의 미세 면역 환경에 대해서는 연구가 많이 되어있지 않으며 위장관 기질 종양 환자에 효과적인 면역항암치료 약제는 없다. 새로운 면역 항암치료의 향후 적용 방법을 모색하기 위하여 위장관 기질종양의 미세 면역환경을 분석하였다.

방법: 본 연구에는 67명의 환자로부터 획득된 80개의 수술 조직이 분석되었다. 분석 수술 조직은 수술 당시의 치료 약제 및 상태에 따라 다음과 같이 구분되었다: 티로신 키나아제 치료 전 군(TKI-naïve group) (n=20); 이마티닙에 종양 진행 하였고, 다른 약제 치료를 받지 않은 환자 군 (IM-PD group, n=30); 및 이마티닙에 종양 진행하였고, 수니티닙 혹은 레고라페닙을 투약 후 수술을 시행한 환자 군 (IM-PD/SU-treated group, n=30). 일곱 색의 다중 면역 형광 염색은 80개의 모든 조직에 시행이 되었고, RNA sequencing 분석 및 면역-관련 유전자 발현 분석은 총 29개의 수술조직을 대상으로 시행되었다. (TKI-naïve [n=10], IM-PD [n=14], and IM-PD/SU-treated group [n=5]).

결과: TKI-naïve group에서 mm^2 당 면역 세포의 중위수 (사분위수 범위, interquartile range [IQR])는 다음과 같다.: CD3+, 79.2 (22.4-434.5); CD3+/CD8+, 6.7 (1.5-75.6); CD3+/FoxP3+, 4.4 (0.3-28.3); CD68+/CD204+, 2.3 (1.1-41.1); CD68+/CD204-, 8.7 (2.0-20.1); CD3+/PD1+, 0.6 (0-2.0); 및 CD3+/TIM3+, 0.2 (0-2.5). IM-PD/SU-treated group에서 mm^2 당 면역 세포의

중위수 (사분위수 범위, interquartile range [IQR])는 다음과 같다.: CD3+, 302.9 (63.4-502.9); CD3+/CD8+, 38.6 (8.9-105.4); CD3+/FoxP3+, 34.0 (6.6-59.7); CD68+/CD204+, 25.2 (6.4-54.2); CD68+/CD204-, 9.6 (4.0-28.9); CD3+/PD-1+, 2.3 (1.0-3.7); 및 CD3+/TIM3+, 1.8 (0-12.7). 조절 T 세포 (regulatory T cells; CD3+/FoxP3+), M2 타입의 대식세포 (macrophages; CD68+/CD204+), PD-1 양성 T 세포 (CD3+/PD-1+), 및 TIM3 양성 T 세포 (CD3+/TIM3+)는 IM-PD/SU-treated group에서 그 수가 증가되어 있었다 (각, *P*=0.047, *P*=0.023, *P*=0.016, and *P*=0.002).

IM-PD/SU-treated group에서는 종양침윤 T-세포/종양세포 비율 (CD3+ cells per DOG-1+ cells, *P*=0.03); PD-1양성 T-세포/전체 T 세포 비율 (CD3+/PD-1+ per CD3+, *P*=0.002); PD-1 양성 세포독성 T 세포/전체 T 세포 비율 (CD8+/PD-1+ per CD3+, *P*=0.007); PD-L1양성 T 세포/전체 T 세포 비율 (CD3+/PD-L1+ per CD3+, *P*=0.005); 조절 T 세포/전체 T 세포 비율 (CD3+/FoxP3+ per CD3+, *P*=0.006); 및 PD-1 양성 종양세포/전체 종양세포 비율 (DOG-1+/PD-1+ per DOG-1+, *P*=0.01) 이 증가 되어 있었다. IM-PD group과 비교하여 IM-PD/SU-treated group에서는 세포독성 T 세포/전체 T 세포 비율 (CD3+/CD8+ per CD3+; *P*=0.07) 및 TIM3양성 T 세포/전체 T 세포 비율 (CD3+/TIM3+ per CD3+; *P*=0.03)이 증가되어 있었다. IM-PD/SU-treated group에서는 M2 타입의 대식세포가 TKI-naive group (*P*=0.049)에 비하여 유의하게 증가되어 있었다.

RNA sequencing 분석에서, IM-PD/SU treated group에서 *FoxP3* 및 *TIM3* 의 발현이 각각 TKI-naive group 및 IM-PD group에 비하여 증가된 경향을 보였다 (P=0.11 및 P=0.06). *TIGIT* 발현은 IM-PD/SU-treated group에서 IM-PD group에 비하여 유의하게 증가되어 있었다 (P=0.01).

결론: 티로신 키나아제 치료를 받지 않거나, 이마티닙에만 노출이 되었던 위장관 기질 종양과 비교하였을 때 수니티닙 혹은 레고라페닙등과 같은 혈관 생성 억제 항암제에 치료를 받은 종양에서 면역 세포의 종양 침투가 증가 되어 있었고 면역 억제 표현형이 두드러졌다. 본 연구의 결과를 고려하였을 때 혈관 생성 억제 항암제 치료를 받은 환자군이 추후 T 세포 혹은 대식세포를 표적으로 한 면역 항암제 임상 시험의 적절한 타겟으로 생각된다.